Vibronic effects in the 1.4-eV optical center in diamond

Konstantin Iakoubovskii*
Lab. Halfgeleiderfysica, Katholieke Universiteit Leuven, Celestijnenlaan 200 D, 3001 Leuven, Belgium and Department of Physics, King's College London, Strand, London, WC2R 2LS United Kingdom

Gordon Davies
Department of Physics, King's College London, Strand, London, WC2R 2LS United Kingdom
(Received 30 June 2004; published 9 December 2004)

We report optical absorption and luminescence measurements on the 1.4-eV center in diamond. We show that the zero-phonon lines have a temperature-dependent Ni-isotope shift, that the isotopic shifts induced by carbon and nickel are opposite in sign, and that a local vibronic mode is present in the absorption spectrum but not in luminescence. The microscopic properties of the center are successfully analyzed with the Ludwig-Woodbury theory (LWT), revealing that the Ni^+ ion in the 1.4-eV center only weakly interacts with the diamond lattice. The importance of vibronic effects in the LWT analysis is experimentally demonstrated. It is believed that similar effects can account for the discrepancies previously encountered in modeling other $3d^9$ impurities in semiconductors.

DOI: 10.1103/PhysRevB.70.245206 PACS number(s): 61.72.Ji, 71.70.Ej, 71.70.Ch

I. INTRODUCTION

During the last decades there has been a strong interest in Ni-related point defects in diamond, which can be explained by the following reasons.

(1) Most synthetic diamonds are grown by the high-pressure high-temperature (HPHT) technique using a Ni-containing metallic catalyst. Surprisingly, despite the covalent radius of Ni being 57% larger than that of carbon, dispersed Ni atoms are efficiently incorporated in diamond producing a large number of optical and electron spin resonance (ESR) centers. Understanding their properties is important both for science and technology.

(2) The microscopic properties of transition metal related defects in diamond (as well as in other semiconductors), including the energy level structure and the values of the Zeeman splitting factor g, can often be explained within the Ludwig-Woodbury theory[1] (LWT). The important feature of this theory is that its application does not require advanced theoretical training and is thus accessible to a wide range of scientists.

The most studied Ni-related center in diamond is the so-called 1.4-eV system, which dominates the optical spectra of nitrogen-poor and Ni-rich HPHT diamond.[2] This system is characterized by two zero-phonon lines (ZPLs) at $\sim$1.404 and $\sim$1.401 eV originating[3] from transitions between an excited state $ex1$ and two ground states $gr1$ and $gr2$ (see Fig. 1). Both lines are further split by $\sim$0.16 meV into multiplets, in which the line intensities match[3] the natural abundance of the main Ni isotopes (68.27% of ^{58}Ni, 26.1% of ^{60}Ni, 3.59% of ^{62}Ni, and 0.91% of ^{64}Ni), thus revealing that the corresponding defect involves one Ni atom. The uniaxial stress technique applied to the 1.4-eV center revealed trigonal symmetry and assigned the symmetries $\Gamma_{5,6}$, Γ_4, and Γ_4 of the C_{3v} double group[4] to the $gr1$, $gr2$, and $ex1$ states, respectively.[3] Finally, a recent photo-ESR study[5] assigned the 1.4-eV center to Ni^+ ion in the center of a diamond divacancy, where Ni is probably not bonded to the carbon neighbors.

Those three states have been thoroughly characterized by ESR (Ref. 6) (NIRIM2 center) and magneto-optical techniques.[3,7,8] As a result, spin $S=1/2$ was assigned to all those states, and the associated g factors werededuced as $g_{gr1,\parallel}=2.329(5)$, $g_{gr1,\perp}<0.1$;[6] $g_{gr2,\parallel}=1.93(2)$;[8] $g_{ex1,\parallel}<0.01$,[8] $g_{ex1,\perp}=2.5(1)$.[7]

A remarkable property of the 1.4-eV center is that it is exclusively incorporated into the $\langle 111\rangle$ growth sectors of HPHT diamond, and that within the [111] sector, most defects are aligned parallel to the [111] growth direction, but not to the other equivalent trigonal axes.[2] Preferential orientation is observed for the associated NIRIM2 ESR center as well.[6]

In order to explain the unusual anisotropy of the g values and the energy level structure of the 1.4-eV center, the LWT has been employed.[7] This theory successfully explained the rather unusual g_{gr1} and g_{ex1} values and the relative positions of the $gr1$, $gr2$, and $ex1$ states. It also predicted the positions of the higher-lying excited states $ex2$ and $ex3$ (Fig. 1) as 1.50

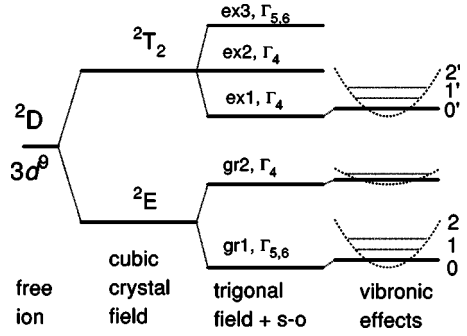

FIG. 1. Schematic diagram of a $3d^9$ ion in a cubic crystal undergoing different perturbations from left to the right: T_d crystal field, trigonal field, spin-orbit coupling, and vibronic coupling. The latter is illustrated for a specific vibrational mode, coupling to which affects differently the involved electronic states. The vertical (energy) scale is severely distorted for presentation purposes.

and 1.52 eV above the ground state $gr1$, and estimated the $g_{gr2,\|}$ value to be in the range 1.67–1.79. However, further magneto-optical measurements yielded a rather different value $g_{gr2,\|}=1.93(2)$,[8] and the predicted excited states $ex2$ and $ex3$ have not been identified yet. Moreover, detailed analysis reveals that the reported polarizations of the optical transitions at the 1.4-eV center[2,9] are in conflict with the deduced level symmetries.[3,7] All those inconsistencies are resolved in the present paper, where most properties of the 1.4-eV center are successfully explained within the LWT.

It has been noticed[7] that the properties of the 1.4-eV center in diamond are similar to those of $3d^9$ (or $3d^1$) transition metal ions in solids,[10] such as V^{4+} in SiC, Cu^{2+} in ZnS, CdS, ZnO, BeO, GaN, and other semiconductors. This observation has at least two important consequences: (i) the well-developed analysis of the $3d^9$ configuration[7,11] can be applied to the 1.4-eV center in diamond and (ii) understanding the properties of the 1.4-eV center can assist modeling other $3d^9$ impurities in solids. In particular, it is recognized that the LWT successfully predicts most properties of $3d^9$ ions in the first approximation, but there remain deviations between the calculated and observed values.[10] Such deviations are commonly attributed to Jahn-Teller effects[10] and other alternatives are rarely considered. In this work, on the example of the 1.4-eV center in diamond, it is experimentally demonstrated that simple vibronic effects, which are not accounted for by the LWT, and which do not necessarily imply presence of Jahn-Teller distortions, can naturally explain some of the LWT failures.

II. EXPERIMENTAL DETAILS

A large number of HPHT diamonds have been studied, but most results were obtained on samples A, B, C, and D; those samples should be considered as representative, but by no means unique. Preliminary measurements revealed that the exact positions of the 1.4-eV lines depend on the strain in the sample, which was revealed by the line broadening. Therefore, samples with sharpest 1.4-eV lines were selected for this study. Sample A is a $[1\bar{1}1]$-oriented plate, laser cut perpendicular to the $[1\bar{1}1]$ direction, as shown by the dashed line in Fig. 2. Sample B is a [110]-oriented plate, laser-cut from the middle of a whole crystal. The 1.4-eV center in samples A and B could be studied in a single $[1\bar{1}1]$ growth sector, viewing along the $[1\bar{1}1]$ (sample A) or [110] (sample B) directions (see Fig. 2). Samples C and D are uncut HPHT crystals. Sample C exhibits the sharpest 1.4 eV lines. Sample D is 100% enriched in ^{13}C isotope (natural abundance of ^{13}C is 1.1%). The 1.4-eV ZPL lines, but unfortunately not the vibronic sideband, in sample D were just strong enough for absorption measurements. Therefore, the absorption from the vibronic sideband of the 1.4-eV center in sample D was recorded using not a conventional absorption routine, but the more sensitive technique of photoluminescence excitation (PLE).

Optical absorption measurements were performed with a commercial IFS-66 Bruker Fourier-transform spectrometer (resolution 0.03 meV), equipped with a He flow cryostat and a linear polarizer. Cathodoluminescence (CL) was excited by a 40-keV electron beam in a home-built setup equipped with a nitrogen-cooled North Coast Ge detector and a nitrogen cryostat. PLE spectra were measured at 77 K with a 250 W tungsten halogen lamp and a double 0.5 m monochromator in excitation and a single 0.25 m monochromator with a Si diode in detection.

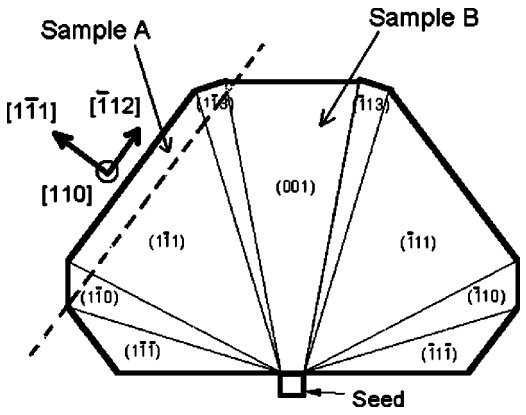

FIG. 2. Schematic drawing of a (110) cross section of a typical HPHT diamond crystals showing the main crystallographic sectors and indicating the sites from which samples A and B were cut.

III. EXPERIMENTAL RESULTS AND PRELIMINARY ANALYSIS

A. Optical features of the 1.4-eV center

Figure 3 presents optical absorption, PLE and CL spectra from the 1.4-eV center, all measured at 77 K. Rather important here is the PLE spectrum. It reveals that all the prominent features observed in the absorption spectrum, and marked by numbers in Fig. 3, do belong to the 1.4-eV center. There is a significant difference between the absorption spectrum and the mirror reflected PL spectrum, however. As discussed later, this difference mostly originates not from vibronic or Jahn-Teller effects, but from extra excited states.

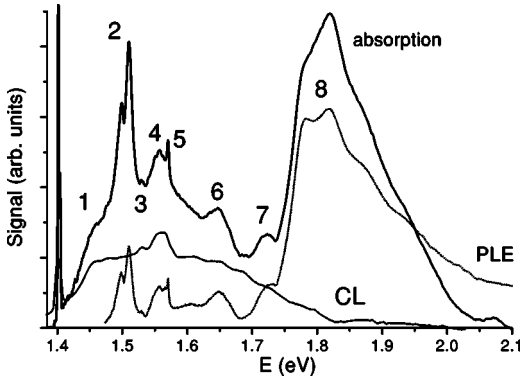

FIG. 3. Optical absorption, CL and PLE spectra from the 1.4-eV center in the HPHT diamond sample B, all recorded at 77 K. The CL spectrum is mirror reflected relatively to the 1.404 eV energy. Numbers indicate the prominent spectral features discussed in the text.

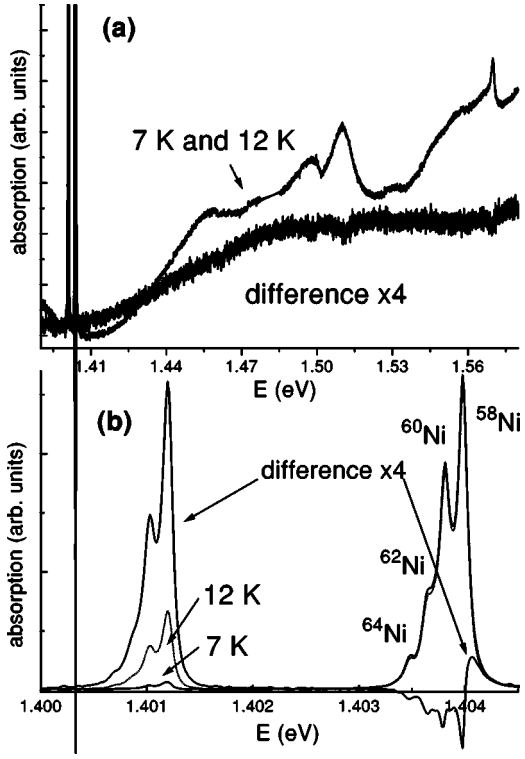

FIG. 4. Optical absorption spectra measured at 12 and 7 K from sample B, and their difference multiplied by 4. Panel (b) shows the details of the 1.4-eV doublet for the wider range spectrum (a). Note that the vertical scale of panel (b) is ~10 times coarser than that of panel (a). The narrow multiplet structure in panel (b) originates from the Ni isotopic structure (natural abundance). The curves for 7 and 12 K in panel (a) and right part of panel (b) are undistinguishable in this presentation.

Comparison of the absorption spectrum and mirror reflected PL spectrum identifies features 1, 3, and 4 seen in absorption at ~1.46, 1.53, and 1.56 eV, respectively, as vibronic modes and suggests that the doublet 2 at 1.501 and 1.513 eV and features 6, 7, and 8 at ~1.65, 1.72, and 1.8 eV, respectively, are not of vibronic origin.

The 1.4-eV center is associated with two ZPLs at 1.401 and 1.404 eV, and in the analysis of the vibronic sideband it is important to identify each feature with a particular ZPL. This is especially important for feature 5, whose distance to the ZPLs is close to the 165 meV cutoff of the diamond phonon spectrum. This task is facilitated by Fig. 4. The 1.401-eV absorption line occurs from the upper ground state *gr*2 (Fig. 1). In the specific temperature range 7–12 K the intensity of the 1.401-eV peak varies significantly while that of the 1.404-eV line remains almost unchanged. Therefore, by plotting in Fig. 4 the difference between the 12 and 7 K absorption spectra, magnified by 4 to approximately equalize the ZPL line intensities, one can compare the vibronic sidebands of the 1.401 and 1.404 eV lines. Rather importantly, Fig. 4(a) reveals that the 1.401 eV line is coupled exclusively to a broad band centered at ~1.5 eV, and not to the sharper features 1–5 (see Fig. 3).

Note that the difference spectrum of Fig. 4(b) exhibits a Ni isotope structure of the 1.401-eV line, which appears to be different from the Ni isotope structure of the 1.404-eV line shown in the same figure. The differences are caused by the temperature dependence of the Ni isotopic splitting discussed later (Fig. 5), to signal noise magnified by subtraction of two weak signals, and to the strong absorption in the 1.404-eV line necessary for this measurement.

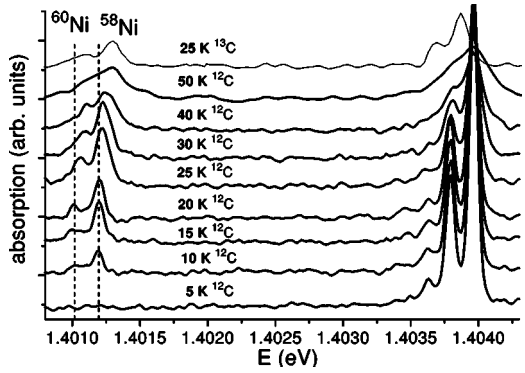

FIG. 5. Optical absorption spectra measured at indicated temperatures from samples C (natural carbon abundance) and D (100% ^{13}C). The multiplet structure originates from the Ni isotopic structure (natural abundance), and the vertical dashed line merely assist the observation of its temperature-induced shift. The spectra are offset for clarity. Spectra for samples C and D are labeled as ^{12}C and ^{13}C, respectively.

B. Ni and carbon isotope effects on the 1.4-eV center

The Ni isotope splitting of both the 1.401- and 1.404-eV lines, shown in Fig. 4(b), is only partially resolved in sample B. Better-resolved spectra, measured in absorption, in the temperature range 5–50 K, are presented in Fig. 5. Thermal line broadening precluded accurate measurements at higher temperatures. This figure brings an important and rather unusual observation. Although both the 1.404- and 1.401-eV lines shift towards lower energies upon increase in Ni mass, the shift is larger for the 1.401-eV line and it is *temperature dependent* for the 1.401-eV, but not for the 1.404-eV line.

The top spectrum of Fig. 5 presents an absorption spectrum from ^{13}C diamond. Because of the weakness of the absorption lines in that diamond, the ZPL doublet could only be reliably recorded at 25 K. Comparison of the spectra of Fig. 5 reveals that the 1.401- and 1.404-eV lines exhibit different behavior upon carbon and Ni isotopic substitutions, which can be summarized as follows.

(i) The 1.401-eV line shifts by 0.18 meV (at 10 K) towards *lower* energies upon substituting ^{60}Ni for ^{58}Ni, and by 0.07 meV towards *higher* energies upon substituting ^{13}C for ^{12}C.

(ii) The 1.404-eV line shifts towards lower energies upon increasing either the carbon *or* the Ni mass. However, the shift is larger for Ni isotopic substitution (0.165 meV) than for carbon substitution (0.10 meV) despite the smaller relative mass change for Ni (60/58) than for carbon (13/12).

(iii) The low-temperature value of the ZPL splitting *increases* from 2.77 to 2.78 meV for the $^{60}Ni/^{58}Ni$ substitution and *decreases* to 2.57 meV upon $^{13}C/^{12}C$ substitution.

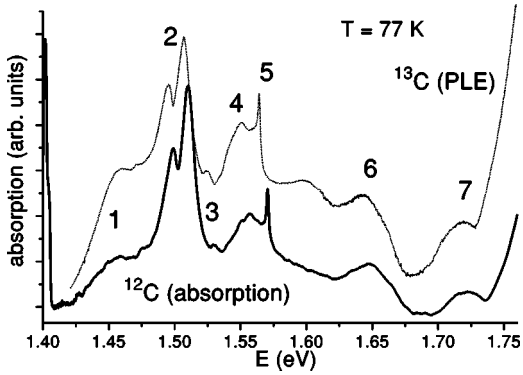

FIG. 6. Absorption spectrum from the sample B (1.1% ^{13}C) and PLE spectrum sample D (100% ^{13}C), both measured at 77 K.

The carbon isotope effect on the other absorption features of the 1.4-eV center is demonstrated in Fig. 6. The analysis of the corresponding spectra reveals that while features 6, 7, and 8 (not shown) do not significantly shift upon substituting ^{13}C for ^{12}C, features 2–5 move towards lower energies. The largest shift, of −6.6 meV, is observed for the peak 5.

C. Polarization properties of the 1.4-eV center

Polarization properties of the 1.4-eV center were analyzed in samples A and B using light linearly polarized along or perpendicular to [111] growth direction. Representative absorption spectra are plotted in Fig. 7. The observed polarizations, together with the proposed assignment of the electronic transitions, symmetry of the involved phonon, and polarizations, predicted by the group theory,[4] are summarized in Table I. Several spectral features in Fig. 7 are polarized thus revealing that the 1.4-eV centers exhibit a preferential orientation, however, most important is the (almost) ideal linear polarization of the doublet at 1.501 and 1.513 eV. It reveals that the preferential polarization of the 1.4-eV centers is (nearly) perfect. The lines at 1.501 and 1.513 eV, which from the temperature-dependence measurements have been shown to occur from the *gr*1 ground state, have the opposite polarisation to the 1.404-eV zero-phonon line from that ground state.

Most spectrometers polarize the light they transmit. The strong polarization dependence of the optical absorption (and luminescence[2]) of the 1.4-eV center naturally explains the variations in its spectral shape that have been reported in the literature.[2,9]

Note that polarized spectra, which look very similar to those of Fig. 7, have already been reported.[2,9] However, the polarization directions are specified differently. For example, spectrum A of Fig. 7 corresponds to spectrum B in those previous studies,[2,9] and vice versa. It seems likely that the polarizations were misprinted in those previous studies for at least two reasons.

(i) The spectra B and C are rather similar, which would be impossible if spectrum B were recorded with the polarizer along the $[1\bar{1}\bar{1}]$ axis. Here, sample A (spectrum C) acts as an extra control, as by its design (see Sec. II and Fig. 2), the optical beam passing normal to its surface is automatically polarized perpendicular to the $[1\bar{1}\bar{1}]$ growth direction.

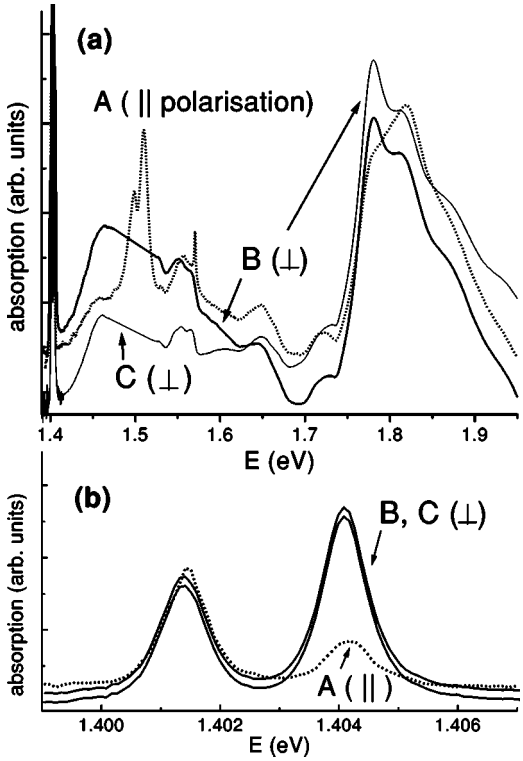

FIG. 7. Absorption spectra measured at 77 K with linearly polarized light in different polarization arrangements. Curve A—sample B, [110] view, $[1\bar{1}\bar{1}]$ polarization (along the growth direction); curve B—sample B, [110] view, $[\bar{1}12]$ polarization (perpendicular to the growth direction); curve C—sample A, $[\bar{1}\bar{1}1]$ view, any polarization in the $(1\bar{1}\bar{1})$ plane (perpendicular to the growth direction). Panel (b) shows the details of the 1.4-eV doublet for the wider range spectrum (a)

(ii) The previously measured polarizations of the intense features[2,9] are just the opposite to those predicted from the level symmetries (see Table I).

IV. ANALYSIS

A. Optical features of the 1.4-eV center

Previous studies of the 1.4-eV center[3,7,8] were primarily concentrated on the ZPL doublet and its perturbation by uniaxial stress and magnetic field, while the vibronic structure remained unexplored. On the contrary, in this and the following sections, we shall focus on identifying the predicted[7] excited states *ex*2 and *ex*3 and on the vibronic and polarization properties of the 1.4-eV center.

The features 1, 3, and 4 (see Fig. 3) have already been assigned to the vibronic modes at the 1.4-eV center in Sec. III A. Therefore, we shall start with the analysis of the yet unidentified features 2, 5–8. Features 6–8 will be of minor importance for the analysis as compared to features 2 and 5, which could be tentatively attributed to the higher-lying excited states $(ex4, 5, \ldots)$ coupled to a vibronic side band (feature 8) and broadened by some, as yet undetermined mechanism.

TABLE I. The proposed assignment of some of the absorption features, as labeled in Fig. 3, at the 1.4 -eV center. The last column presents polarizations predicted by the group theory (Ref. 4).

Label	Energy (eV)	Observed polarization	Electronic transition	Involved phonon	Predicted polarization
	1.401	$\pi+\sigma$	$\Gamma_4 \rightarrow \Gamma_4$		$\pi+\sigma$
	1.404	σ	$\Gamma_{5,6} \rightarrow \Gamma_4$		σ
1	1.46	σ	$\Gamma_{5,6} \rightarrow \Gamma_4$	Γ_1	σ
2	1.501	π	$\Gamma_{5,6} \rightarrow \Gamma_4$		σ
2	1.513	π	$\Gamma_{5,6} \rightarrow \Gamma_{5,6}$		π
3	1.53	$\pi+\sigma$	$\Gamma_{5,6} \rightarrow \Gamma_4$	Γ_3	$\pi+\sigma$
4	1.56	$\pi+\sigma$	$\Gamma_{5,6} \rightarrow \Gamma_4$	Γ_3	$\pi+\sigma$
5	1.571	π	$\Gamma_{5,6} \rightarrow \Gamma_4$	Γ_3	$\pi+\sigma$

The appearance of features 4 and 5, situated near the high-energy cutoff ($1.404+0.165=1.569$ eV) of the one-phonon vibronic spectrum, is unusual, but not unique to the 1.4-eV center. It has been already observed for the H2 center[12] and the single interstitial[13] in diamond, and interpreted as an optical phonon (feature 4) and a local vibrational mode (LVM) (feature 5) situated just beyond the one-phonon spectrum. The absence of the LVM in luminescence is explained by the standard electron-phonon coupling model (see right part of Fig. 1) as follows.[14]

1. The electron-phonon coupling

In the first approximation, the electron-phonon coupling at each electronic state of the 1.4-eV center can be considered as a sum over noninteracting vibronic modes. Every mode is characterized by its frequency ν, which defines the curvature of the electronic potentials in Fig. 1 as a function of the vibrational coordinate(s). Each potential well contains n vibronic energy levels, $n=0,1,2,\ldots$, with energies $h\nu\left(n+\frac{1}{2}\right)$. At low temperatures, only those absorption transitions are active which originate from the lowest level $n=0$, and only the 0-0′ transition contributes to the ZPL. Here (un)primed numbers correspond to the (ground) excited state, respectively. Upon heating, transitions 1-1′, 2-2′, etc., start contributing to the ZPL as well. If the potentials are identical in each electronic state for a given vibrational mode then this mode will induce neither isotopic nor thermal shift of the ZPL. However, in practice, the curvature of the potential differs in various electronic states. This observation is commonly interpreted as the effect on the vibrational potential of the redistribution of the electron density in different electronic states,[14] and it shifts the ZPL upon changing the temperature or the effective mass of the mode (isotopic substitution). The electron density is more diffuse in the excited states for most defects in diamond, reducing the vibrational frequencies. Consequently, most ZPLs in diamond exhibit a blueshift, by some 4 meV, upon substituting ^{13}C for ^{12}C or on cooling the sample.[14] However, for some vibrational modes, such as the LVM of the H2 center,[12] it appears that the ground state is more diffuse than the excited state. As a result, the LVM is well observed in absorption, but, when measured in luminescence, the LVM energy becomes smaller, the mode merges with the diamond phonon continuum, and consequently broadens, and therefore virtually disappears from the luminescence spectrum.[12]

It is important to note that the vibrational mode, responsible for the isotopic shift of the ZPL, may be unobservable in the vibronic sideband. Indeed, this mode could exhibit relatively strong 0-0′, 1-1′, 2-2′, etc., transitions contributing to the ZPL, but not the 0-1′, 0-2′, etc., transitions appearing in the vibronic sideband.

Another important remark concerns the difference between the isotopic and thermal shift of the ZPL. All modes involving a certain type of atom, independent of the mode frequency, contribute to the corresponding isotopic shift by affecting the 0-0′ transition. However, the thermal shift requires excitation of 1-1′, 2-2′, etc., transitions via thermal population of the 1, 2, etc., states. Consequently, only the low-energy (<80 meV) modes dominate the thermal shift of the ZPL at temperatures below 300 K.

2. Local vibrational mode at the 1.4-eV center

The vibronic model outlined in the previous section will be used in the analysis of the 1.4-eV center. First, we shall apply it to the feature 5 in Fig. 3. This feature is present in absorption, but not in luminescence and therefore could well be assigned to an excited state at the 1.4-eV center. However, we would note a remarkable similarity of all its properties and those of the LVM of the H2 center.[12] Those properties include the phonon energy (167 meV in both cases), characteristic line shape, and the low-energy shift upon substituting ^{13}C for ^{12}C by the amount $167\times(1-\sqrt{12/13})=6.6$ meV. Note that this large negative shift is typical for a carbon-related vibronic feature, but has never been observed yet for a ZPL in diamond. Therefore, we attribute the feature 5 to a LVM at the 1.404 eV ZPL rather than to an electronic transition. To be observable in the π polarization (Table I), the LVM must have Γ_3 symmetry. The absence of this LVM in luminescence can be attributed to the mode softening in the ground state. Therefore, we may conclude that the vibrational potential for this mode is softer in the ground state than in the excited state.

3. The excited states ex2 and ex3

Although the features 2 and 5 apparently exhibit similar properties—both are situated close to the one-phonon spec-

trum of the 1.404 eV ZPL, shift towards the lower energies upon substituting ^{13}C for ^{12}C (see Fig. 6), and are not observed in luminescence (Fig. 3)—the doublet 2 cannot be of purely vibronic origin for at least three reasons.

(i) The integral intensity of feature 2 is rather large, larger than that of the 1.4-eV ZPL doublet. Therefore, if feature 2 were a vibronic sideband, it should exhibit[14] strong high-energy harmonics, but none are observed.

(ii) The narrow-line doublet shape would be rather unusual for a vibrational mode situated within the one-phonon diamond spectrum.

(iii) Contrary to the high-energy feature 5, there is no obvious reason for the absence of the strong, low-energy (only 0.1 eV away from the ZPL) doublet 2 in luminescence.

The energies of the lines 2 (1.501 and 1.513 eV) are rather close to those predicted for the excited states *ex*2 and *ex*3 (1.50 and 1.52 eV).[7] Therefore, considering the above arguments [(i)–(iii)], we assume that the doublet 2 does not have a vibronic origin, and attribute it to electronic transitions from the *gr*1 state to the excited states *ex*2 and *ex*3. The large width of the doublet lines may be caused by the lifetime of the *ex*2 and *ex*3 states being short ($\approx 5\times 10^{-14}$ s, a few periods for typical vibrations in diamond), and to the vibronic coupling between the *ex*2 and *ex*3 states and the *ex*1 state. The latter coupling could also contribute to the low-energy shift of the lines 2 upon the $^{13}C/^{12}C$ substitution (Fig. 6).

In Table I, the polarization of the LVM feature 5 is predicted to be $\pi+\sigma$, but π polarization is observed. However, the polarizations in Table I are predicted from the group theory arguments,[4] which reveal whether a transition is allowed in a certain polarization, but cannot assess the associated intensity. The intensity calculations require the analysis of the full Hamiltonian of the 1.4-eV center and lie beyond the scope of this paper. The weak 1.501 eV component of doublet 2 is detected with π polarization, but is predicted to have σ polarization; we cannot explain this discrepancy.

B. Isotopic shift of the zero-phonon lines

Another important application of the vibronic theory outlined in Sec. IV A 1 is to the carbon and Ni isotopic shifts of the 1.401- and 1.404-eV lines. This theory naturally accounts for the high-energy (or low-energy) isotopic shifts of the 1.4-eV ZPLs, as well as their temperature dependence (see Fig. 5), by coupling to appropriate carbon or Ni-related vibrational modes exhibiting more (or less) curvature in the vibrational potential in the excited state than in the ground state. Note that the temperature-dependent Ni isotope shift has been previously observed[15] for $CdS:Ni^{2+}$; however, no detailed explanation has been provided.

The analysis of the isotopic shifts reveals that the 1.4-eV system is unusual in that it exhibits different changes in curvature of the vibrational potentials in the ground and excited states for different vibrational modes.

(i) The Ni-related modes shift the 1.401- and 1.404-eV lines towards lower energies with increasing Ni isotope mass (see Fig. 5). A similar behavior is observed for the 1.404-eV line upon the $^{13}C/^{12}C$ substitution. Therefore, we may conclude that all the corresponding vibrational modes exhibit a stiffer vibrational potential in the excited state than in the ground state.

(ii) A similar asymmetry in the vibrational potential has been deduced for the carbon-related LVM at 1.571 eV in Sec. IV A 2.

(iii) In contrast, the modes responsible for the high-energy shift of the 1.401-eV line with increasing temperature or carbon isotope mass (Fig. 5) correspond to a softer effective potential in the excited state than in the ground state.

The vibronic theory of Sec. IV A 1 also accounts for the different temperature shifts of the dominant ^{58}Ni and ^{60}Ni components of the 1.401-eV line observed in Fig. 5 as follows. The heavier ^{60}Ni isotope should be associated with a lower-frequency mode, for which the 1-1′, 2-2′, etc., transitions will be activated and start to contribute to the 0-0′ transition (1.401-eV ZPL) at lower temperatures compared to the lighter ^{58}Ni isotope. Indeed, Fig. 5 reveals that the lowest energy line at 1.401 02 eV, which corresponds to the ^{60}Ni isotope, starts shifting at lower temperatures than the 1.401 20-eV ^{58}Ni line.

One would intuitively expect the difference in the thermal shift between the ^{60}Ni and ^{58}Ni isotopes to be small, of the order[14] $\exp[-a/(kT\sqrt{60})]-\exp[-a/(kT\sqrt{58})]$, where kT is the Boltzmann temperature factor and a is a constant. The magnitude of this difference, however, strongly depends on the contribution of the other modes. If the latter contribution (nearly) cancels the ^{58}Ni isotope shift then the relative changes upon substituting ^{60}Ni for ^{58}Ni could be significant. A clear example of such cancellation could be seen in the absence of the temperature shift of the 1.404-eV line in Fig. 5.

C. Analysis of the 1.4-eV center with the Ludwig-Woodbury theory

Having identified the excited states *ex*2 and *ex*3 at the 1.4-eV center (Sec. IV A 3), we can reanalyze the 1.4-eV center with the LWT. We shall start with a brief outline of the theory of the $3d^9$ electronic configuration.

When an interstitial Ni^+ ion is placed into the diamond lattice, the cubic crystal field splits the ^2D Ni term into the ^2E and $^2T_2$ states separated by the distance Δ (see Fig. 1). The trigonal perturbation or the spin-orbit coupling, or their combination split the $^2T_2$ state in first order into Γ_4, Γ_4, and $\Gamma_{5,6}$ levels. Here "first order" refers to the expansion series in the small parameters $(K,\lambda)/\Delta$ [see Eq. (1) later]. In contrast, neither the trigonal perturbation nor the spin-orbit coupling split the ^2E level when acting alone.[7] However, when applied together, they do split the ^2E state into the Γ_4 and $\Gamma_{5,6}$ levels in second order. The energy positions (all in meV) and some of the g factors of the derived five states can be expressed as[7,11]

$$E_{gr2} = 4K'\lambda_\parallel'/\Delta = 2.77,$$

$$g_{gr1,\parallel} = 2 - 4k_\parallel'\lambda_\parallel'/\Delta - 8k_\parallel'K'/\Delta = 2.33,$$

$$g_{gr2,\parallel} = 2 - 4k_\parallel'\lambda_\parallel'/\Delta + 8k_\parallel'K'/\Delta = 1.93, \qquad (1)$$

$$E_{ex1} = \Delta + K/2 + \lambda_{\|}/4 - A/2 = 1404,$$

$$E_{ex2} = \Delta + K/2 + \lambda_{\|}/4 + A/2 = 1501,$$

$$E_{ex3} = \Delta - K - \lambda_{\|}/2 = 1513,$$

$$g_{ex1,\|} = (2 + k_{\|})(\lambda_{\|}/2 - 3K)/A - k_{\|} = 0,$$

$$g_{ex1,\perp} = 1 + (\lambda_{\|}/2 - 3K - 2k_{\perp}\lambda_{\perp})/A = 2.5,$$

$$A = \sqrt{(\lambda_{\|}/2 - 3K)^2 + 2\lambda_{\perp}^2}, \quad (2)$$

with the accompanying set of constraints

$$\lambda_{\|,\perp}, \lambda'_{\|,\perp} < 0,$$

$$E_{gr2} > 0,$$

$$0 < k'_{\|}, k_{\|,\perp} \leqslant 1,$$

$$(K, K', \lambda, \lambda') \ll \Delta. \quad (3)$$

Here λ is the anisotropic spin-orbit coupling constant, K is the trigonal field parameter, k is the orbital reduction factor, primed and unprimed values refer to the $^2T_2$ and ^2E states, respectively, and E_{gr1} is set to zero. All the energy values (Δ, λ, K) are taken from the present work and expressed in meV. The g values have been summarized in the Sec. I.

Using Eqs. (2), the constraints (3) can be modified as

$$0.075 \leqslant k_{\|} \leqslant 1,$$

$$0.84 \leqslant k_{\perp} \leqslant 1,$$

$$-18.2 \leqslant K \leqslant -11,$$

$$-44.3 \leqslant \lambda_{\|} \leqslant -58.8,$$

$$-64.7 \leqslant \lambda_{\perp} \leqslant -68.6. \quad (4)$$

The last set of constraints yields a number of important results.

(1) Both $\lambda_{\|}$ and $\lambda_{\perp}$ are automatically larger than the free ion value $\lambda_0 = -75$ meV, as is expected within the LWT. However, the deviations from λ_0 are relatively small, revealing that (i) the electron density in the 1.4-eV center is mostly localized at the Ni^+ ion; (ii) the bonding and Jahn-Teller effects, which tend to reduce the spin-orbit splitting, are weak.

(2) The value of λ is anisotropic. This result explains the differences between the positions of the *ex*2 and *ex*3 states deduced in this study and those predicted previously[7] using the same set of equations, but assuming an isotropic λ.

(3) From the $\lambda_{\perp}$ and $k_{\perp}$ values we can already anticipate that k is close to 1 and that $\lambda \sim \lambda_0$.

Unfortunately, Eqs. (2) are underdetermined and we have to introduce a further approximation. If we assume a reasonable[11] relationship $\lambda_{\|}/\lambda_{\perp} = k_{\|}/k_{\perp}$ then the parameters of the excited state can be deduced as

$$\lambda_{\|} = -49(1),\ \lambda_{\perp} = -67(1),\ K = -16(1),$$

$$k_{\|} = 0.64(1),\ k_{\perp} = 0.88(1),\ \Delta = 1475(5), \quad (5)$$

where all energies are in meV. While the LWT yields rather reasonable parameters for the excited $^2T_2$ state, the agreement for the ^2E state is worse: Eqs. (1) yield $K = -28$ meV, $\lambda'_{\|} = -36$ meV, and an unreasonable value $k' = 1.3 > 1$. However, assuming $\lambda_{\|}/\lambda_0 = k_{\|}$ we obtain reasonable values of $K' = -43$ meV, $\lambda'_{\|} = -56$ meV, and $k'_{\perp} = 0.74$, but then E_{gr2} is 7.5 meV, instead of the experimental value $E_{gr2} = 2.77(1)$ meV.

Such deviation in the E_{gr2} value is commonly observed for $3d^9$ impurities and is usually accounted for by Jahn-Teller effects and a poorly described off-set parameter D_0.[10] Note, that within the LWT the energy levels are independent on the isotopic mass. However Figs. 5 and 6 show that the energy level positions at the 1.4-eV center do depend on the isotopic mass and consequently that the vibronic effects do contribute to the LWT energies including E_{gr2}. In particular, the analysis in the previous sections reveals that vibrational modes do exhibit different frequencies when coupled to different electronic states of the 1.4-eV center. Consequently, vibronic modes of the 1.4-eV center should bring different contributions to the energies the electronic states. The contribution δ to the E_{gr2} value can be estimated, e.g., from the carbon isotopic shift of the ZPL doublet splitting d as $\delta \sim d/[1 - \sqrt{(12/13)}] \approx 4$ meV—a value, which is comparable to the difference $7.5 - 2.8 = 4.7$ meV between the E_{gr2} value calculated with the LWT and measured experimentally. In particular, a slightly asymmetric coupling to a vibrational mode, as depicted in the right part of Fig. 1, would reduce the E_{gr2} value thus explaining the deviation between the experiment and the earlier LWT analysis.

V. CONCLUSIONS

In this work, the Ni-related 1.4-eV center in diamond has been thoroughly characterized by optical absorption and luminescence. A number of interesting vibronic effects have been observed and explained within the simple vibronic theory.[14] Those effects include temperature dependent Ni isotope shift, opposite isotopic shifts for different carbon and Ni-related vibronic modes, and the presence of a local vibrational mode in absorption, but not in luminescence. Detection of the LVM at the 1.4-eV center will be essential in theoretical modeling of its microscopic structure.

Successful identification of the two extra excited states at the 1.4-eV center allowed a detailed analysis of its microscopic properties using the LWT. The theory successfully explained the parameters of the $^2T_2$ excited states yielding values for the anisotropic spin-orbit coupling constant λ, the trigonal field K, and the anisotropic orbital reduction factor k, Eq. (5). Those parameters reveal that (i) the electron density in the 1.4-eV center is mostly localized at the Ni^+ ion; and (ii) the bonding and Jahn-Teller effects are weak at this center.

When analyzing the ground state with the LWT, a deviation has been found between the observed and calculated

values of the ground ^2E state splitting—a discrepancy rather common for $3d^9$ impurities in different solids.[10] However, analysis of the vibronic properties allowed this deviation to be assigned to vibronic effects and in Sec. IV C we estimated the ground ^2E state parameters.

We suggest that similar vibronic effects can possibly account for the difficulties previously encountered in modeling other $3d^9$ impurities in semiconductors.

ACKNOWLEDGMENTS

The authors are indebted to H. Kanda (NIMS, Japan), A. Taylor (DTC Research Center), and I. Kiflawi for provision and preparation of samples. K.I. is grateful to J. M. Baker for illuminating discussions, to A. T. Collins for experimental advice, and to the Belgian FWO for financial support.

*Electronic address: kostya.iak@fys.kuleuven.ac.be

[1] G. W. Ludwig and H. H. Woodbury, Phys. Rev. Lett. **5**, 98 (1960).
[2] A. T. Collins, J. Phys.: Condens. Matter **1**, 439 (1989).
[3] M. H. Nazare, A. J. Neves, and G. Davies, Phys. Rev. B **43**, 14 196 (1997).
[4] M. H. Bartl, E. C. Fuchs, K. Gatterer, H. P. Fritzer, M. Betinelli, and A. Speghini, J. Solid State Chem. **167**, 386 (2002).
[5] K. Iakoubovskii, Phys. Rev. B (to be published).
[6] J. Isoya, H. Kanda, and Y. Uchida, Phys. Rev. B **42**, 9843 (1990).
[7] P. W. Mason, F. S. Ham, and G. D. Watkins, Phys. Rev. B **60**, 5417 (1990), and references therein.
[8] J. Maes, K. Iakoubovskii, M. Hayne, A. Stesmans, and V. Moshchalkov, J. Phys. D **37**, 1102 (2004).
[9] S. C. Lawson, H. Kanda, and M. Sekita, Philos. Mag. B **68**, 39 (1993).
[10] T. Telahun, U. Scherz, P. Thurian, R. Heits, A. Hoffman, and I. Broser, Phys. Rev. B **53**, 1274 (1996).
[11] R. E. Dietz, H. Kamimura, M. Sturge, and A. Yariv, Phys. Rev. **113**, 1559 (1963).
[12] S. C. Lawson, G. Davies, A. T. Collins, and A. Mainwood, J. Phys.: Condens. Matter **4**, 3439 (1992).
[13] H. E. Smith, G. Davies, M. E. Newton, and H. Kanda, Phys. Rev. B **69**, 045206 (2004).
[14] G. Davies, Rep. Prog. Phys. **44**, 787 (1981).
[15] I. Broser, A. Hoffmann, R. Gremer, R. Broser, and E. Birkicht, Phys. Rev. B **33**, 8196 (1986).